Ozone: A potential oxidant for COVID-19 virus (SARS-CoV-2)

Chedly Tizaoui

College of Engineering, Swansea University, Swansea, SA1 8EN, United Kingdom

Corresponding author: Chedly Tizaoui

Email address: c.tizaoui@swansea.ac.uk;

Postal address: College of Engineering, Bay Campus, Swansea University, Swansea, SA1 8EN, United Kingdom

Tel: +44(0) 1792 606841

Abstract

Currently, no medicine has demonstrated efficacy in treating the ongoing pandemic COVID-19 caused by SARS-CoV-2 virus. Being a potent oxidant, ozone is lethal against most bacteria and viruses found in water, or on surfaces and aerosols. Ozone has also been successfully used to treat several viral diseases such as Ebola and HIV Hepatitis B and C. Using molecular modelling, this study evaluated the reactivity of ozone towards representative key molecules in the structure of SARS-CoV-2. The results show that ozone is able to attack the proteins and lipids of the virus's spikes and envelope, particularly the amino acids tryptophan, methionine and cysteine, and the fatty acids, arachidonic acid, linoleic acid and oleic acid. Ozone also attacks the N-glycopeptides of the spike protein subunits 1 and 2, though at lower reactivity. Disruption of the structure of SARS-CoV-2 could inactivate the virus, suggesting that ozone could be an effective oxidant against COVID-19 virus. If incorrectly applied, ozone is toxic and contact with the respiratory tract must be avoided.

Keywords: ozone; SARS-CoV-2; COVID-19; coronavirus; severe acute respiratory syndrome.

1. Introduction

The highly infectious 2019 novel coronavirus disease (COVID-19) is caused by a new coronavirus (SARS-CoV-2) belonging to the family of severe acute respiratory syndrome (SARS) viruses. This virus has high transmission rate and has so far infected all countries in the world. SARS-CoV-2 affects severely the respiratory system of infected people and can lead, according to the World Health Organisation's updated daily data, to about 7% death in infected cases, (as of 15 May 2020). People who suffer from underlining health conditions are most vulnerable. The virus spreads through direct inhalation of infected droplets, or through contact with contaminated surfaces and objects (Chia et al., 2020; Zhen-Dong et al., 2020). The faecal-oral transmission route has also been postulated (Xu et al., 2020b). The virus can remain viable and infectious in aerosols for hours and on surfaces for up to days (van Doremalen et al., 2020). However, recent evidence suggests that the risk of transmission through surface contamination is lower than through the airborne route (Anderson et al., 2020; Centers for Disease Control and Prevention, 2020; Morawska and Cao, 2020; Setti et al., 2020). Currently there is no vaccine nor a specific treatment for the disease, though research is at speed for developing, testing, mass-producing and distributing specific medication and vaccine for COVID-19. People have to social engineer themselves through social-distancing and stay-at-home measures to avoid exposure to the virus. Standard hygiene measures including hand washing and mouth covering when coughing and sneezing are the first defence against SARS-COV-2 as recommended by the World Health Organisation and governments across the world.

Given its strong oxidising power, ozone is suggested here as an oxidising agent that can potentially inactivate and destroy SARS-CoV-2. This is justified by not only the fact that ozone is a strong oxidising agent but also by the fact that SARS-CoV-2 is an enveloped virus, which is particularly vulnerable to oxidation attack. Ozone can attack viruses at various points of their structure causing damage to the virus's integrity while making them enable to reproduce through oxidising the viral capsid and the genetic material. Although any of the virus's structure could potentially be attacked by

ozone, the structure that has most of the double bonds or groups with high electronic density will be most vulnerable to ozone oxidation. The following summary provides state of knowledge on ozone inactivation of viruses while emphasising the potential of ozone as a strong oxidant to inactivate and destroy SARS-COV-2.

2. Method

The search engines PubMed, Web of Science, Google Scholar were searched irrespective of language and time using combinations of the key words: ozone; medical ozone; COVID-19; SARS-CoV-2; coronavirus; SARS; severe acute respiratory syndrome; MERS; middle east respiratory syndrome; virus inactivation; antimicrobial. In addition, a volume of original dated published references from the International Ozone Association and handbooks were consulted. The semi-empirical PM6 method was used in Gaussian 16 to carry out a rapid molecular optimisation and frequency calculations, thereby obtaining the electronic structure of molecules, providing ozone reactivity towards molecules identified in the structure of SARS-CoV-2.

3. Results and Discussion

3.1 Ozone: a versatile virucidal

Ozone is an excellent oxidising agent and due to its ability to kill almost all kinds of bacteria and viruses, it has been extensively used to disinfect water, wastewater, air, and food, and has gained applications in the energy, laundry and health sectors (Langlais et al., 1991; Khadre et al., 2001; Rice, 2002; Tseng and Li, 2008; Rice et al., 2009; Zanardi et al., 2016; Tizaoui, 2017). Early research on ozone has mainly focused on inactivating waterborne viruses and have demonstrated that relatively low ozone concentration (~1mg/L) and short contact time (~1min) (i.e. CT~1mg.min/L) were sufficient to inactivate 99% of viruses, such as rotaviruses, parvoviruses, feline calicivirus, and hepatitis A virus (Akey and Walton, 1985; Tseng and Li, 2008; Hirai et al., 2019). A more recent viral inactivation kinetic data show that ozone was highly effective against enteric viruses with second-order ozone inactivation

rate constants ranging from 4.5×10^5 to 3.3×10^6 $M^{-1}.s^{-1}$ (Wolf et al., 2018). Evidence has also shown that ozone is effective against airborne and on-surface viruses (Tseng and Li, 2008; Hudson et al., 2009; Hirneisen and Kniel, 2013), though the kinetics are slightly lower than in aqueous solutions (Bialoszewski et al., 2011). However, with appropriate control of ozone dose and air humidity (relative humidity: RH~80%), the virus inactivation rates increase substantially making ozone an attractive and rapid method for inactivating airborne and on-surface viruses (Hudson et al., 2009; Hirneisen and Kniel, 2013).

Although the water industry is the largest user of ozone gas, medical ozone, produced and applied under strict conditions, is an excellent therapy (Bocci, 2002; Viebahn-Hänsler et al., 2016). The virucidal and bactericidal properties of ozone in health have been recognised since World War one, when ozone was applied to disinfect wounds and mustard gas burns (Viebahn-Hänsler, 2007). If incorrectly applied, ozone can be toxic to humans, but when it is applied appropriately (Bocci, 2002; Viebahn-Hänsler et al., 2012), ozone is effective to treat a multitude of diseases including wounds, ulcers, circulatory disorders, viral diseases (e.g. Ebola), and even cancers (Bocci, 2002; Elvis and Ekta, 2011; Rowen, 2019). In fact, ozone is not a strange molecule to the human body since our immune system naturally produces it as part of its defence strategy against invading microbial pathogens (Wentworth et al., 2003; Loscalzo, 2004; Wanjala et al., 2018). As part of its molecular defence network, salivary antibodies also catalyse ozone formation to kill microorganisms efficiently in the oral cavity (Fábián et al., 2012). The action mechanisms of ozone in the medical field include inactivation of microorganisms, stimulation of oxygen metabolism and activation of the immune system (Elvis and Ekta, 2011). As an oxidation therapy, medical ozone is administered through various routes including ozonized saline solution, autohemotherapy, extravascular blood oxygenation-ozonation, body exposure to ozone gas, rectal insufflation etc. (Viebahn-Hänsler, 2007; Bocci et al., 2011; Schwartz, 2016; Moreno-Fernandez et al., 2019). Methods that administer ozone directly to the infected part (e.g. by bagging or application of ozonated aqueous solutions on a wound) result in oxidative attack

of the pathogens. However, when ozone is supplied to the blood, its direct virucidal activity is not guaranteed due to a protection provided by the antioxidant system in blood or the intracellular viruses become inaccessible to ozone. As ozone is transferred to blood, it instantly reacts with blood biomolecules such as unsaturated fatty acids to generate reactive oxygen species and lipid oxidation products such as hydrogen peroxide, ozonides, and lipid peroxides. These ozone reaction products will act as ozone messengers responsible for stimulating the biological and therapeutic effects of ozone instead of a direct attack of the viruses by ozone (Bocci et al., 1998; Bocci, 2006; Zanardi et al., 2016). Ozone is toxic when breathed; thus it must not be inhaled.

3.2 Mode of action of ozone against viruses

Due to its high oxidising power, ozone is particularly lethal against viruses, both enveloped and non-enveloped (Murray et al., 2008). Although the mode of action of ozone against viruses is yet to be fully clarified, ozone is likely to react with viruses through the direct molecular ozone reaction mechanism and/or indirectly through reactive oxygen species (ROS) such as $^{\bullet}OH$, $O_2^{\bullet-}$ and H_2O_2 produced as a result of ozone decomposition. In addition, the reactions between ozone and its ROS with the constituents of the virus structure including lipids, proteins and amino acids could lead to the formation of other ROS including reactive radicals ($RCOO^{\bullet}$) which further propagate oxidation through a chain reaction. Ozone reacts readily with several biological compounds in the order of preference: lipids (particularly polyunsaturated fatty acids)>antioxidants>cysteine-rich proteins>carbohydrates (Bocci, 2002). Murray et al. (2008) showed that ozone inactivates viruses through lipid and protein peroxidation followed by subsequent damage to the lipid viral envelope and protein capsid. Kim et al. (1980) showed that ozone (<1mg/L for 5 seconds) inactivated bacteriophage f2 in water and have found that ozone attacked the phage coat, breaking the protein capsid into subunits while Roy et al. (1981) have concluded that damage to the viral nucleic acid was the major cause of poliovirus 1 inactivation by ozone. Genome attack by ozone has also been recently confirmed by Young et al. (2020). Thus, ozone

and its ROS are capable to attack the virus at different sites of its structure destroying it and making it inactive to infect.

3.3 Potential inactivation of SARS-CoV-2 with ozone

SARS-CoV-2 is reported to belong to the β-B group of coronaviruses and has a diameter in the range 50 to 200 nm (Zhou et al., 2020) (approximately 500 times larger than the size of an ozone molecule (Table S1)). Similar to other coronaviruses, SARS-CoV-2 has a structure consisting of a core genetic material surrounded by an envelope of protein spikes resembling a crown (Xu et al., 2020a). Figure 1(a) shows a model representation of SARS-CoV-2 structure. The core genetic material is a single positive-sense RNA genome protected by a nucleocapsid (N), while the viral envelope is created by three structural proteins: spike (S), envelope (E), and membrane (M). The genome encodes these four major structural proteins (i.e S, E, M and N), which are all required to produce a structurally complete virus. The spike S-protein is made of two subunits S1 and S2 and is responsible for initiating the infection events through a strong binding of subunit S1 to the human angiotensin-converting enzyme 2 (ACE2) receptor (Xu et al., 2020a). The binding affinity of S1 to ACE2 was found to be 10 to 20 times higher than that of SARS-CoV (the virus that was responsible for the outbreak of SARS in 2003) (Wrapp et al., 2020), which could explain the high infectivity and transmissibility of SARS-COV-2 as compared to SARS-CoV. After binding of the subunit S1 to the receptor ACE2 on the host cell, the subunit S2 forms a six-helix bundle, serving to bring into close proximity the viral and cellular membranes for fusion and infection.

Ozone oxidation of the S-proteins could therefore inhibit the infection process. As shown in Figure 1(b), ozone and its ROS could also attack the envelope of the virus and if ozone and its ROS are able to penetrate the envelope, they could attack the genome capsid and its RNA making the virus unable to reproduce. Currently, there are no studies on ozone inactivation of SARS-CoV-2 but in a study conducted in China following the 2003 SARS outbreak, ozone was found effective to kill SARS-CoV

virus in water within minutes (Jia-min et al., 2004). This suggests that ozone could be a potential lethal oxidant against SARS-CoV-2 since both viruses come from the same group and have similar structures; sharing 79.6% of the genome structure and having 89.8% identical sequence of the subunit S2 while the S1 subunit of both viruses bind to human ACE2 (Zhou et al., 2020).

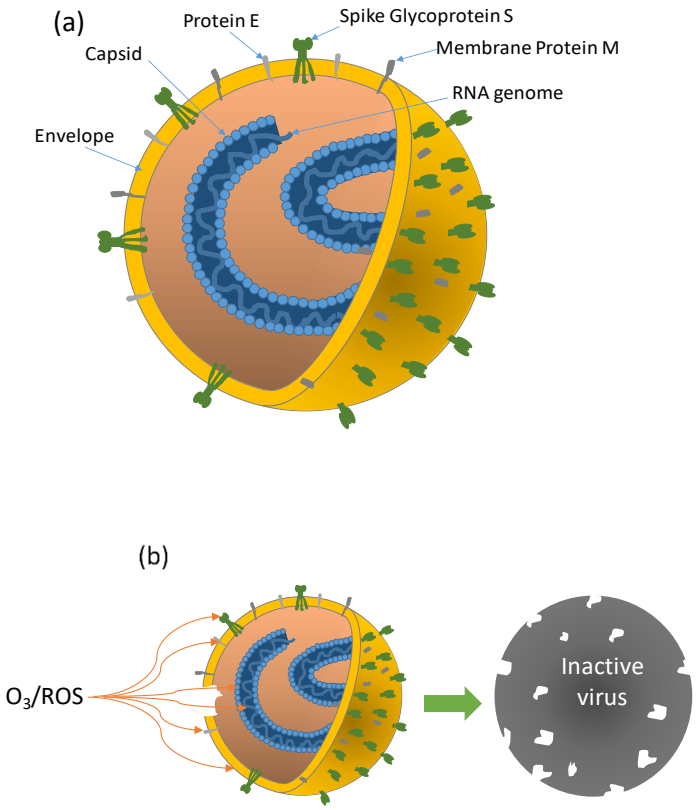

Fig. 1 (a) Structure of SARS-CoV-2; (b) Potential sites for ozone attack leading to inactive virus

The lipid structure of SARS-CoV-2 contains fatty acids, such as arachidonic acid (AA), linoleic acid (LA), palmitic (PA) and oleic acids (OA) (Yan et al., 2019) and is rich in glutamic acid (Cárdenas-Conejo et al., 2020). Particularly, AA and LA have been found to play an important role in the coronavirus infection mechanism (Yan et al., 2019). In addition, amino acids including cysteine and tryptophan are abundant molecules in the corona virus proteins such as those in the spikes and the envelope and are crucial in membrane fusion (Broer et al., 2006). Besides, the amino acid methionine plays an important role in stabilizing protein structure and virus replication (Valley et al., 2012; Svancarova and Betakova,

2018). The glycoproteins in the spikes, which promote entry into cells, are densely decorated by heterogeneous N-linked glycans and are the main target of antibodies (Walls et al., 2020). To evaluate the reactivity of ozone with molecules in the structure of SARS-CoV-2, these fatty acids and amino acids, in addition to representative N-glycopeptides (FSNVTWF (site N61) of spike protein subunit 1 (GS1) and EGVFVSNGTHWFVTQR (site N1098) of spike protein subunit 2 (GS2)) (Shajahan et al., 2020) have been modelled in Gaussian 19 using the semi-empirical PM6 method. Molecules of known reactivity with ozone in the order phenol > methyl benzene > benzene were also modelled for comparison purpose only using the same modelling method (i.e. PM6). The reactivity of ozone was evaluated by calculating the highest occupied molecular orbital (HOMO) energy values for each molecule; molecules with high HOMO react faster with ozone (Naumov and von Sonntag, 2010).

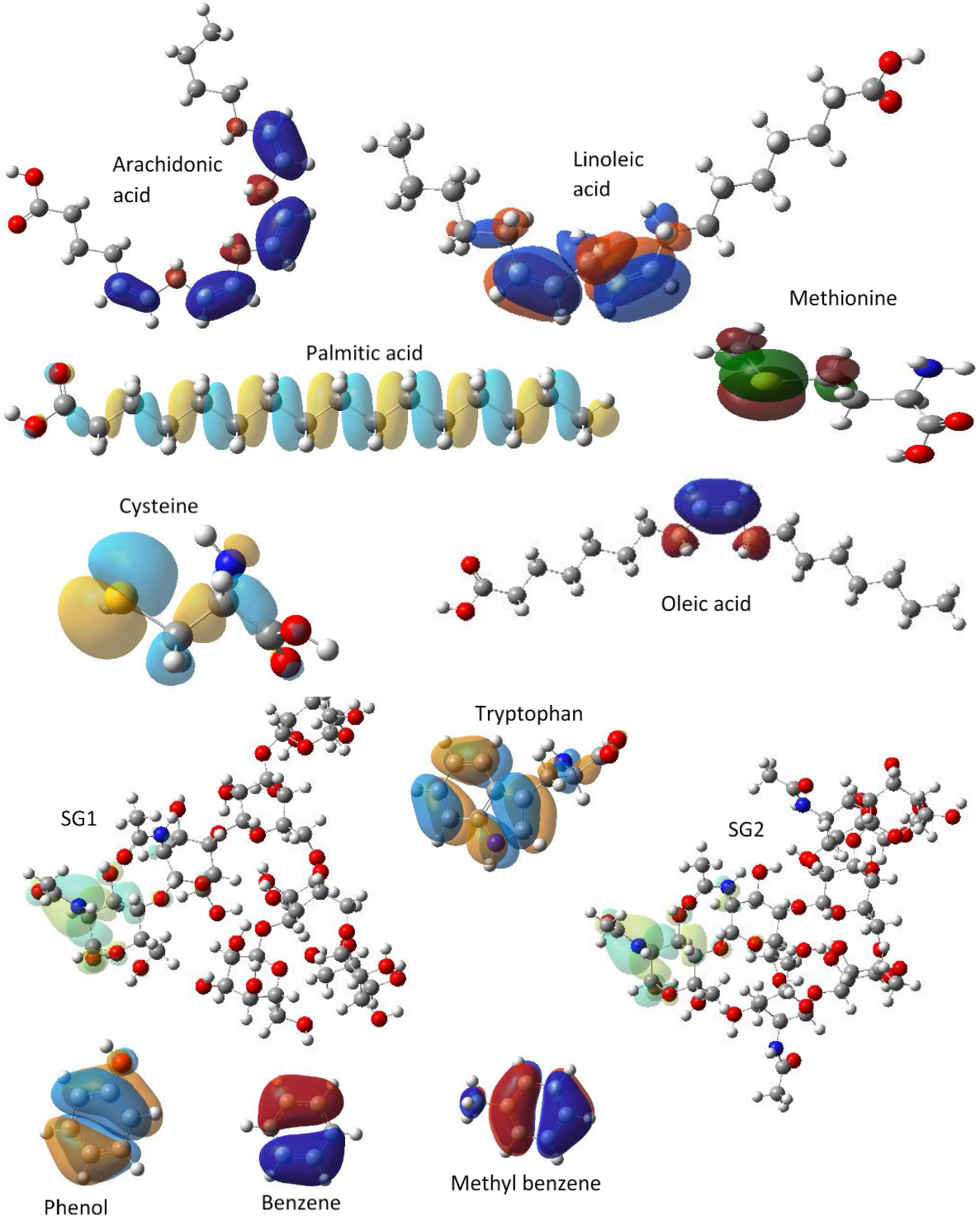

Fig. 2 Computed surface plots of HOMO energy of molecules in SARS-CoV-2 structure. SG1: FSNVTWF (site N61) of spike protein subunit 1 and SG2: EGVFVSNGTHWFVTQR (site N1098) of spike protein

subunit 2 according to Shajahan et al. (2020). Phenol, benzene, and methyl benzene are for comparison only.

Figures 2 and 3 show surface and bar chart plots of the HOMO energies of the studied molecules. Figure 3 shows that ozone has very high reactivity towards the amino acids tryptophan and methionine since they have the highest HOMO energies. According to Figure 3, the HOMO energies of tryptophan and methionine are comparable, indicating that they have similar reactivity with ozone, a result which is in agreement with Sharma and Graham (2010). The high reactivity of ozone towards tryptophan (even higher than phenol) is reasonable since the reaction takes place at the indole ring, which has high electronic density (Figure 2) while methionine's high reactivity is due to the sulphur-methyl thioether group. In their study of methionine oxidation, Choe et al. (2015) showed that methionine was preferentially targeted, with respect to other amino acids, forming predominantly methionine sulfoxide. Ozone reactivity is sensitive to the degree of ionisation of a molecule, which is related to pH. In this study, the simulations were made considering neutral forms of the molecules but to illustrate the importance of pH, simulations were made allowing for the speciation of tryptophan, methionine and cysteine at two pHs (7 and 8). At these pHs, the degree of ionisation of tryptophan and methionine does not change significantly, with both molecules remain in their neutral forms by more than 95% (Figures S1, S2, and S3). However, the degree of ionisation of cysteine changes significantly as pH changes from 7 to 8 as illustrated in Figure S4 and Table S2. When protonated at low pH, cysteine has three acidic hydrogens including carbonyl (-COOH), amino ($-NH_3^+$), and thiol (-SH). As the pH increases, cysteine looses hydrogen ions to solution according to the values of its dissociation constants (Eq. S3 and Figure S4). At the pHs 7 and 8, cysteine exists predominantly in its two forms AH_2 and AH^- at the percentages 94% (AH_2) and 6% (AH^-) at pH7 and 60% (AH_2) and 40% (AH^-) at pH8 (Table S2). The corresponding HOMO energies, calculated by Gaussian 16, of the species AH_2 and AH^- of cysteine are -9.73eV and -4.20eV respectively, indicating that the ionised form of cysteine (AH^-) is particularly very reactive with ozone since its HOMO energy is much higher than

species AH_2. Considering weighted averages, cysteine HOMO energies are calculated and the values are -9.39eV and -7.52eV at pH 7 and 8 respectively (Table S2). Data from Naumov and von Sonntag shows that for each unit increase of the HOMO energy, the rate constant of ozone reaction increases by approximately 4 folds (Naumov and von Sonntag, 2010). Thus at pH8, cysteine is significantly more reactive than at neutral pH. Wolf et al. (2018) have also shown that ozone virus inactivation rate constants increase with increasing pH. On the other hand, both tryptophan and methionine have comparable HOMO energies of -8.81eV and -8.83eV respectively indicating that they have similar reactivity with ozone, which is in agreement with Sharma and Graham (2010). Comparing tryptophan and methionine to cysteine, both appear more reactive towards ozone at pH7 than cysteine since their HOMO energies are higher (Figure 3). However at pH8, due to ionisation thus high HOMO energy, cysteine (-7.52eV) becomes more reactive than tryptophan and methionine (Figure 3), which is in agreement with the results presented by Sharma and Graham (2010).

According to Figure 3 and among the fatty acids, arachidonic acid presents the highest reactivity towards ozone followed by linoleic acid, oleic acid and palmitic acid. This is consistent with the number of unsaturated bonds (UB) in each fatty acid: AA (four UB), LA (two UB), OA (one UB), and PA (zero UB). The three fatty acids AA, LA and OA have lower reactivity than phenol and methylbenzene but higher reactivity than benzene, while PA has the lowest reactivity due to the absence of unsaturated bonds in its molecular structure. Cysteine is also prone to ozone attack at pH 7 with a reactivity higher than benzene but lower than phenol and methyl benzene. On the other hand, the spike protein subunit 2 (GS2) has similar reactivity to benzene while protein subunit 1 (GS1) has slightly lower reactivity, possibly due to the absence of double bonds in their molecular structures. Considering these results, ozone appears effective to attack the amino acids (particularly tryptophan, methionine, and cysteine (at pH8)) and fatty acids (particularly arachidonic acid), thus able to disrupt the protein and lipid structures of the virus, which could lead to its destruction. Since these molecules play key roles in the pathogenesis of coronaviruses (Broer et al., 2006; Yan et al., 2019), their disruption could

also disrupt and inhibit key events in the viral infection mechanism such as virus binding and fusion with the host cell, thus ozone oxidation renders the virus not infective. Besides molecular ozone, radicals produced from its decomposition could cause further damage to the virus's structure, thereby increasing the likelihood of ozone efficacy against this deadly virus.

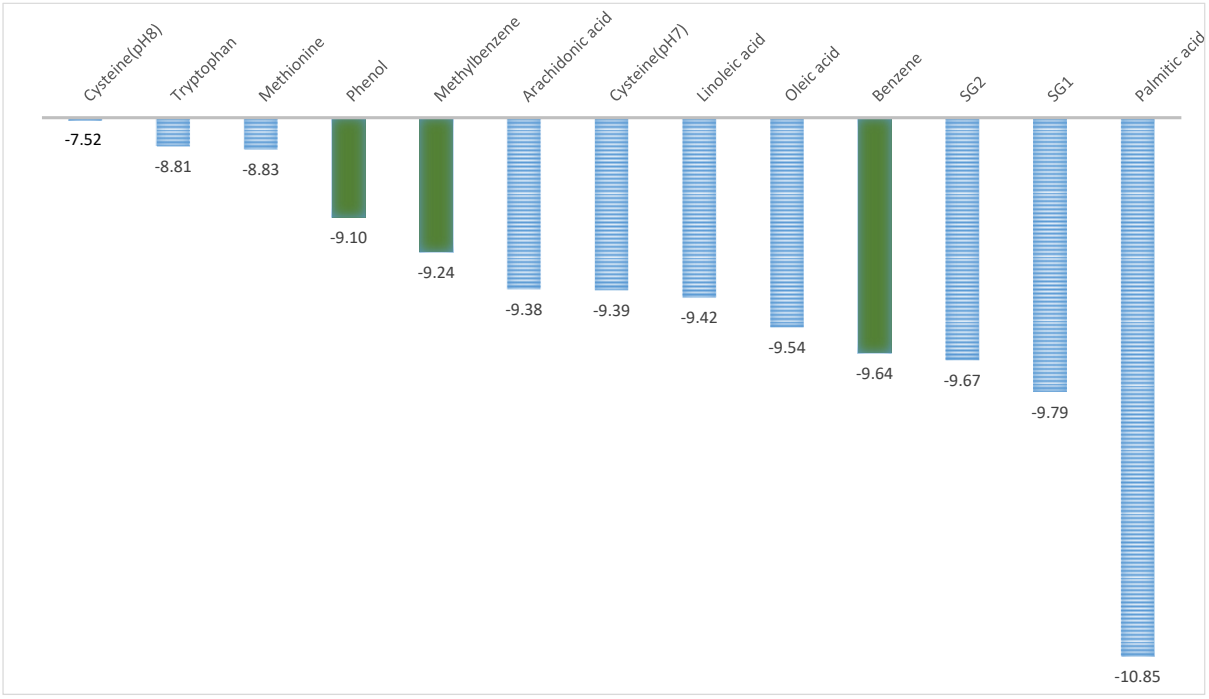

Fig. 3 HOMO energy values (eV) for molecules in SARS-CoV-2 (blue) and comparative molecules (green)

Conclusions

Through molecular modelling, this study showed that ozone could be an affective oxidant against SARS-CoV-2. Ozone could attack the proteins and lipids of the virus's spikes and envelope, thus destroying the integrity of the virus and inhibiting the mechanism by which it infects. Ozone could support the current effort in fighting COVID-19.

Funding

No funding was received for this study.

References

Akey, D.H., and T.E. Walton. 1985. "Liquid-phase study of ozone inactivation of Venezuelan equine encephalomyelitis virus", Applied and environmental microbiology 50(4): 882-886.

Anderson, E.L., P. Turnham, J.R. Griffin, and C.C. Clarke. 2020. "Consideration of the Aerosol Transmission for COVID-19 and Public Health", Risk Analysis 40(5): 902-907.

Bialoszewski, D., A. Pietruczuk-Padzik, A. Kalicinska, E. Bocian, M. Czajkowska, B. Bukowska, and S. Tyski. 2011. "Activity of ozonated water and ozone against Staphylococcus aureus and Pseudomonas aeruginosa biofilms", Medical science monitor : international medical journal of experimental and clinical research 17(11): Br339-344.

Bocci, V., Oxygen-Ozone Therapy: A Critical Evaluation (Dordrecht: Kluwer Academic Publishers 2002)

Bocci, V., G. Valacchi, F. Corradeschi, C. Aldinucci, S. Silvestri, E. Paccagnini, and R. Gerlf. 1998. "Studies on the biological effects of ozone: 7. Generation of reactive oxygen species (ROS) after exposure of human blood to ozone", Journal of biological regulators and homeostatic agents 12(3): 67-75.

Bocci, V., I. Zanardi, and V. Travagli. 2011. "Oxygen/ozone as a medical gas mixture. A critical evaluation of the various methods clarifies positive and negative aspects", Med Gas Res 1(1): 6-6.

Bocci, V.A. 2006. "Scientific and medical aspects of ozone therapy. State of the art", Archives of medical research 37(4): 425-435.

Broer, R., B. Boson, W. Spaan, F.-L. Cosset, and J. Corver. 2006. "Important role for the transmembrane domain of severe acute respiratory syndrome coronavirus spike protein during entry", Journal of virology 80(3): 1302-1310.

Cárdenas-Conejo, Y., A. Liñan-Rico, D.A. García-Rodríguez, S. Centeno-Leija, and H. Serrano-Posada. 2020. "An exclusive 42 amino acid signature in pp1ab protein provides insights into the evolutive history of the 2019 novel human-pathogenic coronavirus (SARS-CoV-2)", Journal of Medical Virology:

Centers for Disease Control and Prevention. 2020. "How COVID-19 Spreads. Available at https://www.cdc.gov/coronavirus/2019-ncov/prevent-getting-sick/how-covid-spreads.html":

Chia, P.Y., K.K. Coleman, Y.K. Tan, S.W.X. Ong, M. Gum, S.K. Lau, S. Sutjipto, P.H. Lee, T.T. Son, B.E. Young, D.K. Milton, G.C. Gray, S. Schuster, T. Barkham, P.P. De, S. Vasoo, M. Chan, B.S.P. Ang, B.H. Tan, Y.S. Leo, O.-T. Ng, M.S.Y. Wong, and K. Marimuthu. 2020. "Detection of Air and Surface Contamination by Severe Acute Respiratory Syndrome Coronavirus 2 (SARS-CoV-2) in Hospital Rooms of Infected Patients", medRxiv: 2020.2003.2029.20046557.

Choe, J.K., D.H. Richards, C.J. Wilson, and W.A. Mitch. 2015. "Degradation of Amino Acids and Structure in Model Proteins and Bacteriophage MS2 by Chlorine, Bromine, and Ozone", Environ Sci Technol 49(22): 13331-13339.

Elvis, A.M., and J.S. Ekta. 2011. "Ozone therapy: A clinical review", Journal of Natural Science, Biology, and Medicine 2(1): 66-70.

Fábián, T.K., P. Hermann, A. Beck, P. Fejérdy, and G. Fábián. 2012. "Salivary defense proteins: their network and role in innate and acquired oral immunity", Int J Mol Sci 13(4): 4295-4320.

Hirai, K., N. Ando, H. Komada, A. Sounai, M. Murakami, and H. Nakayama. 2019. "Investigation of the Effective Concentration of Ozonated Water for Disinfection in the Presence of Protein Contaminants", Biocontrol Sci 24(3): 155-160.

Hirneisen, K.A., and K.E. Kniel. 2013. "Inactivation of internalized and surface contaminated enteric viruses in green onions", International journal of food microbiology 166(2): 201-206.

Hudson, J.B., M. Sharma, and S. Vimalanathan. 2009. "Development of a Practical Method for Using Ozone Gas as a Virus Decontaminating Agent", Ozone-Science & Engineering 31(3): 216-223.

Jia-min, Z., Z. Chong-yi, X. Geng-fu, Z. Yuan-quan, and G. Rong. 2004. "Examination of the efficacy of ozone solution disinfectant in activating SARS virus", Chinese Journal of Disinfection:
Khadre, M.A., A.E. Yousef, and J.G. Kim. 2001. "Microbiological aspects of ozone applications in food: A review", J Food Sci 66(9): 1242-1252.
Kim, C.K., D.M. Gentile, and O.J. Sproul. 1980. "Mechanism of Ozone Inactivation of Bacteriophage f2", Applied and environmental microbiology 39(1): 210-218.
Langlais, B., D. Reckhow, and D. Brink, Ozone in Water Treatment: Application and Engineering (New York: Lewis Publishers, 1991)
Loscalzo, J. 2004. "Ozone — From Environmental Pollutant to Atherogenic Determinant", New England Journal of Medicine 350(8): 834-835.
Morawska, L., and J. Cao. 2020. "Airborne transmission of SARS-CoV-2: The world should face the reality", Environ Int 139: 105730-105730.
Moreno-Fernandez, A., L. Macias-Garcia, R. Valverde-Moreno, T. Ortiz, A. Fernandez-Rodriguez, A. Molini-Estrada, and M. De-Miguel. 2019. "Autohemotherapy with ozone as a possible effective treatment for Fibromyalgia", Acta reumatologica portuguesa:
Murray, B.K., S. Ohmine, D.P. Tomer, K.J. Jensen, F.B. Johnson, J.J. Kirsi, R.A. Robison, and K.L. O'Neill. 2008. "Virion disruption by ozone-mediated reactive oxygen species", J Virol Methods 153(1): 74-77.
Naumov, S., and C. von Sonntag. 2010. "Quantum Chemical Studies on the Formation of Ozone Adducts to Aromatic Compounds in Aqueous Solution", Ozone-Science & Engineering 32(1): 61-65.
Rice, R.G. 2002. "Century 21 - Pregnant with Ozone", Ozone: Science & Engineering 24(1): 1-15.
Rice, R.G., M. Debrum, J. Hook, D. Cardis, and C. Tapp. 2009. "Microbiological Benefits of Ozone in Laundering Systems", Ozone-Science & Engineering 31(5): 357-368.
Rowen, R.J. 2019. "Ozone and oxidation therapies as a solution to the emerging crisis in infectious disease management: a review of current knowledge and experience", Med Gas Res 9(4): 232-236.
Roy, D., P.K. Wong, R.S. Engelbrecht, and E.S. Chian. 1981. "Mechanism of enteroviral inactivation by ozone", Applied and environmental microbiology 41(3): 718-723.
Schwartz, A. 2016. "Ozonized Saline Solution (O3SS): Scientific Foundations", Revista Española de Ozonoterapia 6(1): 121-129.
Setti, L., F. Passarini, G. De Gennaro, P. Barbieri, M.G. Perrone, M. Borelli, J. Palmisani, A. Di Gilio, P. Piscitelli, and A. Miani. 2020. "Airborne Transmission Route of COVID-19: Why 2 Meters/6 Feet of Inter-Personal Distance Could Not Be Enough", International journal of environmental research and public health 17(8):
Shajahan, A., N.T. Supekar, A.S. Gleinich, and P. Azadi. 2020. "Deducing the N- and O- glycosylation profile of the spike protein of novel coronavirus SARS-CoV-2", bioRxiv: 2020.2004.2001.020966.
Sharma, V.K., and N.J.D. Graham. 2010. "Oxidation of Amino Acids, Peptides and Proteins by Ozone: A Review", Ozone: Science & Engineering 32(2): 81-90.
Svancarova, P., and T. Betakova. 2018. "Conserved methionine 165 of matrix protein contributes to the nuclear import and is essential for influenza A virus replication", Virology Journal 15:
Tizaoui, C. 2017. "Guest Editorial: Ozone and Advanced Oxidation for the Water–Energy–Food–Health Nexus", Ozone: Science & Engineering 39(5): 293-294.
Tseng, C., and C. Li. 2008. "Inactivation of surface viruses by gaseous Ozone", J Environ Health 70(10): 56-62.
Valley, C.C., A. Cembran, J.D. Perlmutter, A.K. Lewis, N.P. Labello, J. Gao, and J.N. Sachs. 2012. "The Methionine-aromatic Motif Plays a Unique Role in Stabilizing Protein Structure", Journal of Biological Chemistry 287(42): 34979-34991.
van Doremalen, N., T. Bushmaker, D.H. Morris, M.G. Holbrook, A. Gamble, B.N. Williamson, A. Tamin, J.L. Harcourt, N.J. Thornburg, S.I. Gerber, J.O. Lloyd-Smith, E. de Wit, and V.J.

Munster. 2020. "Aerosol and Surface Stability of SARS-CoV-2 as Compared with SARS-CoV-1", New England Journal of Medicine:
Viebahn-Hänsler, R., The Use of Ozone in Medicine ODREI-Publishers 2007)
Viebahn-Hänsler, R., O.S. León Fernández, and Z. Fahmy. 2012. "Ozone in Medicine: The Low-Dose Ozone Concept—Guidelines and Treatment Strategies", Ozone: Science & Engineering 34(6): 408-424.
Viebahn-Hänsler, R., O.S. León Fernández, and Z. Fahmy. 2016. "Ozone in Medicine: Clinical Evaluation and Evidence Classification of the Systemic Ozone Applications, Major Autohemotherapy and Rectal Insufflation, According to the Requirements for Evidence-Based Medicine", Ozone: Science & Engineering 38(5): 322-345.
Walls, A.C., Y.-J. Park, M.A. Tortorici, A. Wall, A.T. McGuire, and D. Veesler. 2020. "Structure, Function, and Antigenicity of the SARS-CoV-2 Spike Glycoprotein", Cell:
Wanjala, G.W., A.N. Onyango, D. Abuga, C. Onyango, and M. Makayoto. 2018. "Evidence for the Formation of Ozone (or Ozone-Like Oxidants) by the Reaction of Singlet Oxygen with Amino Acids", J Chem: 6.
Wentworth, P., J. Nieva, C. Takeuchi, R. Galve, A.D. Wentworth, R.B. Dilley, G.A. DeLaria, A. Saven, B.M. Babior, K.D. Janda, A. Eschenmoser, and R.A. Lerner. 2003. "Evidence for ozone formation in human atherosclerotic arteries", Science 302(5647): 1053-1056.
Wolf, C., U. von Gunten, and T. Kohn. 2018. "Kinetics of Inactivation of Waterborne Enteric Viruses by Ozone", Environ Sci Technol 52(4): 2170-2177.
Wrapp, D., N. Wang, K.S. Corbett, J.A. Goldsmith, C.-L. Hsieh, O. Abiona, B.S. Graham, and J.S. McLellan. 2020. "Cryo-EM structure of the 2019-nCoV spike in the prefusion conformation", Science 367(6483): 1260-1263.
Xu, X., P. Chen, J. Wang, J. Feng, H. Zhou, X. Li, W. Zhong, and P. Hao. 2020a. "Evolution of the novel coronavirus from the ongoing Wuhan outbreak and modeling of its spike protein for risk of human transmission", Science China Life Sciences 63(3): 457-460.
Xu, Y., X.F. Li, B. Zhu, H.Y. Liang, C.X. Fang, Y. Gong, Q.Z. Guo, X. Sun, D.Y. Zhao, J. Shen, H.Y. Zhang, H.S. Liu, H.M. Xia, J.L. Tang, K. Zhang, and S.T. Gong. 2020b. "Characteristics of pediatric SARS-CoV-2 infection and potential evidence for persistent fecal viral shedding", Nat Med: 9.
Yan, B., H. Chu, D. Yang, K.-H. Sze, P.-M. Lai, S. Yuan, H. Shuai, Y. Wang, R.Y.-T. Kao, J.F.-W. Chan, and K.-Y. Yuen. 2019. "Characterization of the Lipidomic Profile of Human Coronavirus-Infected Cells: Implications for Lipid Metabolism Remodeling upon Coronavirus Replication", Viruses 11(1): 73.
Young, S., J. Torrey, V. Bachmann, and T. Kohn. 2020. "Relationship Between Inactivation and Genome Damage of Human Enteroviruses Upon Treatment by UV254, Free Chlorine, and Ozone", Food and environmental virology 12(1): 20-27.
Zanardi, I., E. Borrelli, G. Valacchi, V. Travagli, and V. Bocci. 2016. "Ozone: A Multifaceted Molecule with Unexpected Therapeutic Activity", Curr Med Chem 23(4): 304-314.
Zhen-Dong, G., W. Zhong-Yi, Z. Shou-Feng, L. Xiao, L. Lin, L. Chao, C. Yan, F. Rui-Bin, D. Yun-Zhu, C. Xiang-Yang, Z. Meng-Yao, L. Kun, C. Cheng, L. Bin, Z. Ke, G. Yu-Wei, L. Bing, and C. Wei. 2020. "Aerosol and Surface Distribution of Severe Acute Respiratory Syndrome Coronavirus 2 in Hospital Wards, Wuhan, China, 2020", Emerging Infectious Disease journal 26(7):
Zhou, P., X.-L. Yang, X.-G. Wang, B. Hu, L. Zhang, W. Zhang, H.-R. Si, Y. Zhu, B. Li, C.-L. Huang, H.-D. Chen, J. Chen, Y. Luo, H. Guo, R.-D. Jiang, M.-Q. Liu, Y. Chen, X.-R. Shen, X. Wang, X.-S. Zheng, K. Zhao, Q.-J. Chen, F. Deng, L.-L. Liu, B. Yan, F.-X. Zhan, Y.-Y. Wang, G.-F. Xiao, and Z.-L. Shi. 2020. "A pneumonia outbreak associated with a new coronavirus of probable bat origin", Nature 579(7798): 270-273.

Supporting Information

Ozone: A potential oxidant for COVID-19 virus (SARS-CoV-2)

Chedly Tizaoui

College of Engineering, Swansea University, Swansea, SA1 8EN, United Kingdom

Contents

Tryptophan:

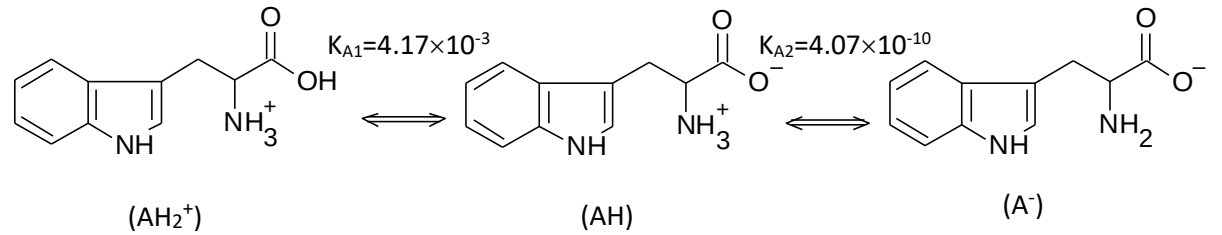

(Eq. S1)

Methionine:

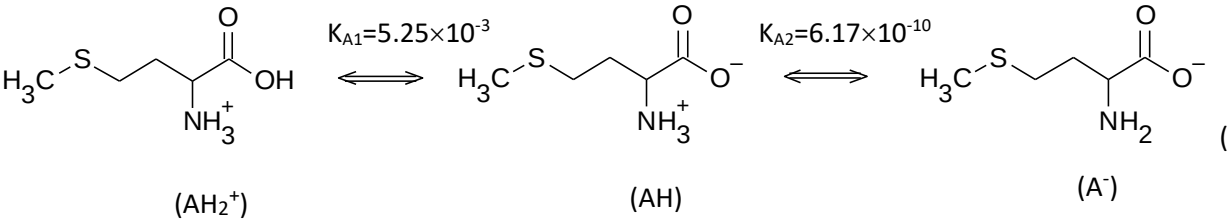

(Eq. S2)

Cysteine:

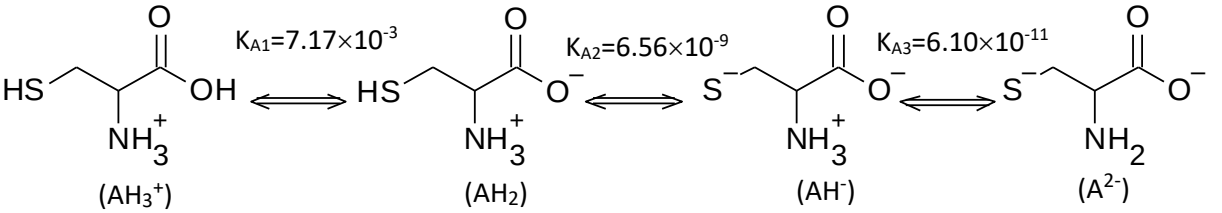

(Eq. S3)

Figure S1: Acid/base dissociation reaction equations for tryptophan, methionine and cysteine. Hydrogen ions resulting from each dissociation reaction are not shown to simplify the equations

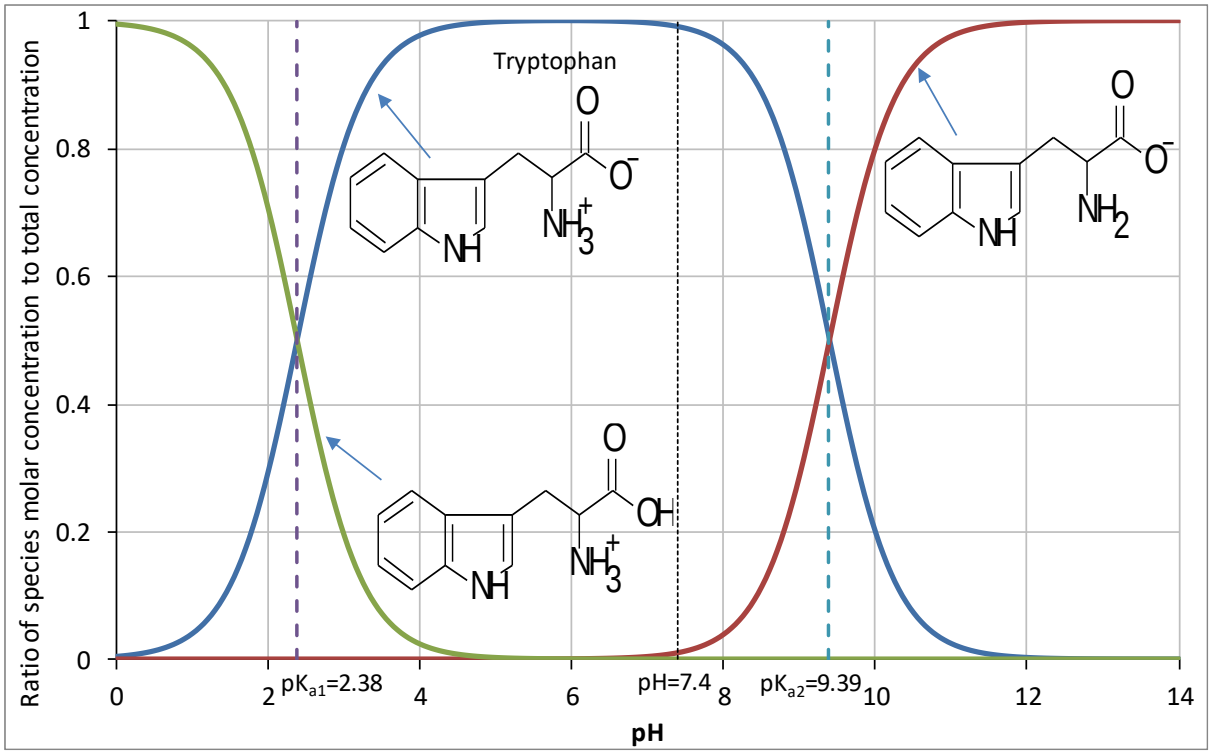

Figure S2: Tryptophan speciation as function of pH

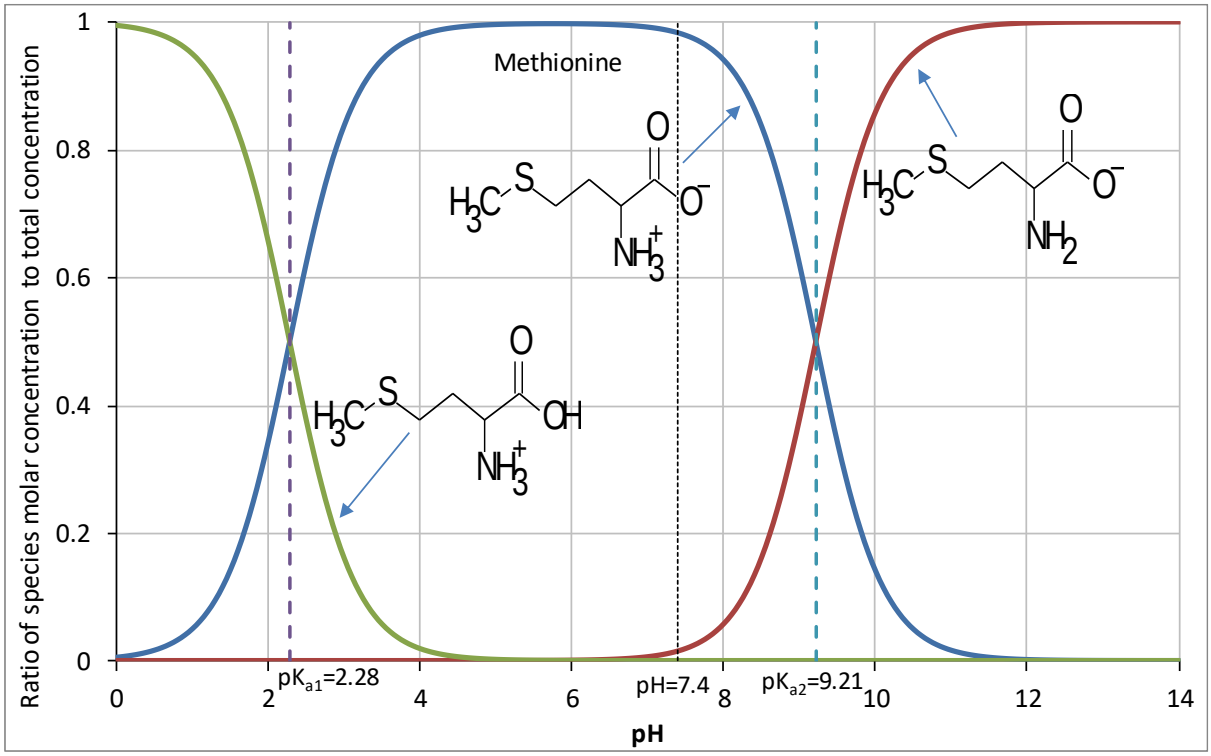

Figure S3: Methionine speciation as function of pH

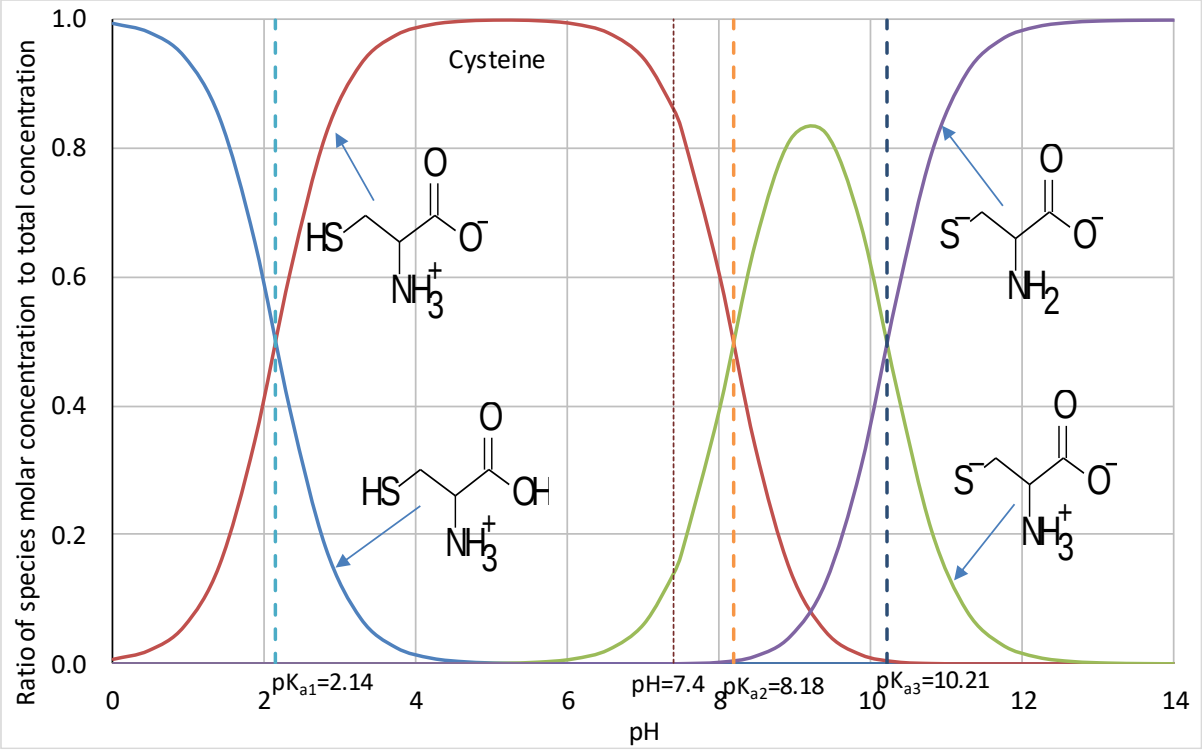

Figure S4: Cysteine speciation as function of pH

Table S1: Size ratio between SARS-CoV-2 and O_3 molecule

Virus diameter range (nm)	50 to 200
selected virus diameter (nm)	110

O_3 molecule size:

α(°)	116.8
L(Å)	1.278
α(rad)	2.04
sin(α/2)	0.85
r(Å)	1.09
d(Å)	2.18

Virus diameter/O_3 diameter	505

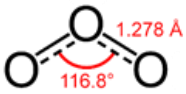

Table S2: Speciation of cysteine at pHs 7 and 8 and the corresponding average HOMO

pH	AH_3^+ (%)	AH_2 (%)	AH^- (%)	A^{2-} (%)	HOMO(eV)
7	0	94	6	0	-9.39
8	0	60	40	0	-7.52

Table S3: Cartesian coordinates of molecular structures

Ozone

0,1

O	0.000000000000	1.088507080000	-0.223218020000
O	0.000000000000	0.000000000000	0.446436030000
O	0.000000000000	-1.088507080000	-0.223218020000

Arachidonic acid

0,1

C	25.051163446000	-6.585804927586	0.000000000000
C	24.458305305670	-7.961238012663	0.000000000000
C	22.927169997697	-7.908000999261	0.000000000000
C	22.323104962068	-9.317591636741	0.000000000000
C	20.824233563838	-9.292771616270	0.000000000000
C	20.054143018394	-10.386915520556	0.000000000000
C	20.580903333279	-11.790364058397	0.000000000000
C	19.510008403519	-12.839688977809	0.000000000000
C	19.746299590188	-14.156604869380	0.000000000000
C	21.114649159439	-14.769212227611	0.000000000000

1	C	21.107633546879	-16.268571668525	0.000000000000
2	C	22.210237619149	-17.026457386050	0.000000000000
3	C	23.607911433984	-16.483882735586	0.000000000000
4	C	24.670192559051	-17.542411158952	0.000000000000
5	C	25.983941827464	-17.288417949259	0.000000000000
6	C	26.578711552440	-15.912754909271	0.000000000000
7	C	28.114916381245	-15.935418212505	0.000000000000
8	C	28.692333126012	-14.515164330752	0.000000000000
9	C	30.231320068486	-14.424177744510	0.000000000000
10	C	30.983706040327	-15.751731013418	0.000000000000
11	O	26.429545328716	-6.685275126515	0.000000000000
12	O	24.537270645976	-5.493980183084	0.000000000000
13	H	24.837089492939	-8.525154361862	0.881641149362
14	H	24.837089492939	-8.525154361862	-0.881641149362
15	H	22.570467139598	-7.337169990272	-0.882353543093
16	H	22.570467139598	-7.337169990272	0.882353543093
17	H	22.683942202443	-9.884185808006	0.885079642494
18	H	22.683942202443	-9.884185808006	-0.885079642494
19	H	20.369847483842	-8.300683900467	0.000000000000
20	H	18.966407615921	-10.294499036925	0.000000000000
21	H	21.241851205357	-11.937243594875	0.885586058706
22	H	21.241851205357	-11.937243594875	-0.885586058706
23	H	18.485531435938	-12.463961884382	0.000000000000
24	H	18.915912838908	-14.864840878170	0.000000000000
25	H	21.683794521817	-14.402809804695	0.885666013051
26	H	21.683794521817	-14.402809804695	-0.885666013051
27	H	20.120097831367	-16.732615678061	0.000000000000
28	H	22.130198190618	-18.114841326463	0.000000000000
29	H	23.747764326615	-15.821186527517	0.885364956823
30	H	23.747764326615	-15.821186527517	-0.885364956823
31	H	24.306917357721	-18.571053843039	0.000000000000
32	H	26.701804183944	-18.109969122011	0.000000000000
33	H	26.211716848793	-15.349761891011	0.884244925325
34	H	26.211716848793	-15.349761891011	-0.884244925325
35	H	28.480445373908	-16.491218650063	-0.885144251161
36	H	28.480445373908	-16.491218650063	0.885144251161
37	H	28.304047568812	-13.968383409406	0.882016052141
38	H	28.304047568812	-13.968383409406	-0.882016052141
39	H	30.552138776809	-13.834027326557	0.882256926883
40	H	30.552138776809	-13.834027326557	-0.882256926883
41	H	32.067406115650	-15.586116267408	0.000000000000
42	H	30.745800003819	-16.353233588586	0.884700165010
43	H	30.745800003819	-16.353233588586	-0.884700165010
44	H	26.879296449013	-5.799859893099	0.000000000000
45				
46	**Linoleic acid**			
47	0,1			

1	O	13.969901122784	-19.970026629136	0.508850721744
2	C	14.671798545857	-20.158337679389	-0.454982793656
3	O	14.800633201094	-19.161196260772	-1.402655452788
4	C	15.504547703203	-21.335870206818	-0.857920288930
5	C	15.044015369704	-22.611659920905	-0.144330275458
6	C	15.951554860047	-23.798205877869	-0.488748115690
7	C	15.484005003954	-25.076375150974	0.220561166939
8	C	16.389483743696	-26.267891596110	-0.119048502859
9	C	15.920341862650	-27.545308229805	0.590068965354
10	C	16.825281684026	-28.738552146385	0.251965081145
11	C	16.388898869615	-30.002122415745	0.929797080639
12	C	16.994510325500	-31.185828169675	0.780818640647
13	C	18.203367411926	-31.415529070953	-0.075910711228
14	C	18.501711195370	-32.868200638295	-0.298705379985
15	C	19.725716025336	-33.380935591864	-0.464302853877
16	C	20.997758500158	-32.588471694238	-0.449983138462
17	C	22.191432453906	-33.420208606135	0.041297517388
18	C	23.481633903180	-32.590414116135	0.062983160318
19	C	24.675808582978	-33.422286725673	0.551923132255
20	C	25.963574498908	-32.601931650775	0.576627180402
21	H	14.277658134084	-18.347196124891	-1.178861502875
22	H	16.570956246146	-21.116619502135	-0.624936673283
23	H	15.474001077047	-21.463963459942	-1.962891451016
24	H	13.994544180161	-22.839211653846	-0.420129349815
25	H	15.029659101417	-22.442481947178	0.952956309989
26	H	16.997337683855	-23.572090409259	-0.202889371463
27	H	15.965650952054	-23.960447854231	-1.584171800705
28	H	14.438421394516	-25.305345483918	-0.063854551229
29	H	15.468608062891	-24.915724417732	1.316378708321
30	H	17.434537805664	-26.040701920776	0.167512898193
31	H	16.404766049627	-26.429519047155	-1.214275378126
32	H	14.875531989249	-27.774220259062	0.302958335890
33	H	15.905230418396	-27.384653254587	1.685710456308
34	H	17.873509326242	-28.507954520815	0.538041652481
35	H	16.845580085042	-28.893942579151	-0.847937325549
36	H	15.518310557831	-29.909080518472	1.580422978704
37	H	16.626862155258	-32.065631037490	1.311225815214
38	H	18.072430794000	-30.925074547706	-1.067759709049
39	H	19.077694748964	-30.902258513226	0.389066034427
40	H	17.622148025595	-33.513437987130	-0.337824922200
41	H	19.854013625672	-34.450898509269	-0.638597038218
42	H	20.885980964402	-31.683700955166	0.185541237848
43	H	21.196148444518	-32.208145575041	-1.474623460019
44	H	22.325374255868	-34.308084727379	-0.606310903094
45	H	21.977823388674	-33.814045546542	1.054191130947
46	H	23.351219745685	-31.704917985406	0.714325300133
47	H	23.692161692107	-32.191391011503	-0.947789017619

1	H	24.809600713906	-34.307972931705	-0.099611329542
2	H	24.467295214837	-33.820749121858	1.564234848594
3	H	26.809630229240	-33.203911799977	0.926638188754
4	H	26.220373265953	-32.223180146544	-0.419140527346
5	H	25.878512857206	-31.736897933257	1.244095241450
6				
7	**Palmitic acid**			
8	0,1			
9	O	26.212852680939	-9.018190705491	0.452959058797
10	C	7.064037845244	-10.914598260041	-0.006493949570
11	C	8.333599296821	-10.066015348317	-0.024042070781
12	C	9.598601612532	-10.935607332483	-0.000916249491
13	C	10.870880886097	-10.077941131133	-0.018669403376
14	C	12.134621258738	-10.948441061275	0.004488870950
15	C	13.407160235571	-10.090763455622	-0.013278689869
16	C	14.670807384227	-10.961374306718	0.009905315813
17	C	15.943243408191	-10.103554528637	-0.007916109661
18	C	17.206936715257	-10.974094643977	0.015318323260
19	C	18.479099387706	-10.115909337563	-0.002636147384
20	C	19.742887702305	-10.986314203916	0.020730504404
21	C	21.014212601332	-10.127080903909	0.002512743454
22	C	22.278176236871	-10.997331394752	0.026089858566
23	C	23.544490094360	-10.133451500030	0.008843118785
24	C	24.807836917228	-11.001045406283	0.024783445357
25	C	26.043722428487	-10.158516511620	0.094896239826
26	O	27.128329627905	-10.900833523080	-0.331464825396
27	H	6.167054492888	-10.285607934863	-0.023174997107
28	H	7.009310599685	-11.540390027340	0.891493547700
29	H	7.012841098426	-11.582197501639	-0.874062981163
30	H	8.334564010766	-9.377406358870	0.843475392931
31	H	8.338103720207	-9.419225000795	-0.923155625137
32	H	9.595315865173	-11.624714002594	-0.867144709560
33	H	9.591778010685	-11.582933022139	0.896948238428
34	H	10.872574881538	-9.389312602764	0.848155643890
35	H	10.876122420221	-9.431101111687	-0.917088994283
36	H	12.132698339528	-11.637130287187	-0.862283188794
37	H	12.129159967528	-11.595286129741	0.902911254585
38	H	13.408658169689	-9.402053642175	0.853506231396
39	H	13.412207439716	-9.443868248315	-0.911678734157
40	H	14.668910671982	-11.650067488703	-0.856872613123
41	H	14.665392487006	-11.608128728342	0.908405710072
42	H	15.944595016304	-9.414754258382	0.858845751431
43	H	15.948134202241	-9.456648885271	-0.906346596335
44	H	17.204924745169	-11.662859115816	-0.851423687419
45	H	17.201458562791	-11.620696716210	0.913955863258
46	H	18.480107753024	-9.426882517930	0.864062062642
47	H	18.483613058845	-9.468977550832	-0.901132680733

1	H	19.740574898457	-11.675241935006	-0.845956255784
2	H	19.737165711090	-11.632569115266	0.919703834292
3	H	21.014621703149	-9.437485428318	0.869213621343
4	H	21.017830457015	-9.479801732000	-0.896044538128
5	H	22.275915988022	-11.685978583647	-0.841206138987
6	H	22.271275143460	-11.643613905321	0.925409283366
7	H	23.552950596092	-9.443734965536	0.878909521749
8	H	23.549110452138	-9.478228833884	-0.885484511636
9	H	24.848006025876	-11.663055153052	-0.868765969948
10	H	24.798212451206	-11.695657909841	0.894857369690
11	H	27.981178830271	-10.393697061687	-0.293141118162
12				
13	**Oleic acid**			
14	0,1			
15	O	32.171038477092	-14.585126856352	-0.307060839774
16	C	11.562638464087	-15.328919402843	0.569855021259
17	C	13.059857220318	-15.610623044300	0.675335496408
18	C	13.897633629311	-14.417443749552	0.194286736271
19	C	15.400884715212	-14.705822227094	0.302404457325
20	C	16.236846009792	-13.512183853701	-0.178930267803
21	C	17.740433353117	-13.800165556480	-0.071032660649
22	C	18.575110305659	-12.606053058036	-0.552833599969
23	C	20.079374255468	-12.893421521529	-0.445109162808
24	C	20.921001216545	-11.743614988417	-0.909436176924
25	C	22.259236792413	-11.744410113802	-0.915160086524
26	C	23.102717078072	-12.895861961552	-0.457856470488
27	C	24.606335845004	-12.609556440428	-0.576269224088
28	C	25.443214402829	-13.804826066422	-0.101162707392
29	C	26.945814628286	-13.516741527198	-0.220006945958
30	C	27.783920755123	-14.711536761592	0.254849548434
31	C	29.283596761118	-14.417932154985	0.132714635414
32	C	30.122382764874	-15.607144546208	0.613497544326
33	C	31.584988019709	-15.355015347034	0.414693866954
34	O	32.310278365076	-16.202902612559	1.229633639170
35	H	10.973172650588	-16.185532922089	0.915126495969
36	H	11.270971820131	-14.464043708861	1.176449865401
37	H	11.263154098267	-15.119629750061	-0.463367422400
38	H	13.313016176311	-16.511397324448	0.082655123343
39	H	13.320853485214	-15.855354713836	1.723542381965
40	H	13.641975320463	-13.517474653318	0.785880890487
41	H	13.634148108292	-14.172548628773	-0.852562743088
42	H	15.654730270021	-15.606109042260	-0.289727291792
43	H	15.662585872457	-14.950431903116	1.349901403218
44	H	15.982505769568	-12.611889840653	0.413122590694
45	H	15.974588819860	-13.267463002850	-1.226347063228
46	H	17.993941326922	-14.700585811133	-0.663165813402
47	H	18.001914851913	-14.044559481850	0.976600650065

H	18.321728721408	-11.705796714672	0.040028943538
H	18.313817953638	-12.362374049046	-1.600931691573
H	20.331326765077	-13.800264939299	-1.035245193944
H	20.339277099585	-13.143532346082	0.605605141570
H	20.370062566911	-10.868969217677	-1.257354500223
H	22.808422152621	-10.870700845929	-1.267731897156
H	22.844994155424	-13.801558689710	-1.047297278317
H	22.849537798603	-13.146482103213	0.594382366131
H	24.864241742530	-11.709512831620	0.015134297428
H	24.859834140887	-12.365155194980	-1.626241389957
H	25.183951399780	-14.704227828298	-0.692566521850
H	25.188063482914	-14.049336694270	0.948105074460
H	27.203945746540	-12.615818459263	0.370106496414
H	27.199947851125	-13.270940801039	-1.269693506241
H	27.523427263769	-15.610752702929	-0.336818169643
H	27.528682470591	-14.955641161242	1.304481968958
H	29.545501500903	-13.512264788214	0.716145158332
H	29.545133641534	-14.176125990758	-0.918938486314
H	29.841381662362	-16.535004005689	0.066033492340
H	29.916689018491	-15.833417304881	1.683452563108
H	33.291509146194	-16.088087127855	1.128821252526

Cysteine

0,1

C	1.303504418623	0.361151888391	-0.009971461934
C	-0.024583565174	-0.216060491028	-0.517578269196
C	-1.093995618027	0.062786653816	0.545969037327
O	1.729984957480	1.338664892266	-0.872354531301
O	1.933550049950	0.096255496236	0.983412115615
N	0.252871082128	-1.636873837406	-0.810849738482
S	-2.650483193615	-0.694356121417	0.005651288578
H	-1.265751204920	1.154107226864	0.658206555830
H	-0.783288484127	-0.295078402819	1.546305015159
H	-2.723068444800	-1.718055108023	0.881641887872
H	-0.296462800015	0.298293780919	-1.485843895476
H	0.371305994146	-2.184015833289	0.037688574007
H	-0.497623593400	-2.051628717814	-1.358556468334
H	2.607940401751	1.730408573303	-0.614020109667

Tryptophan

0,1

C	0.039500974220	-0.610879403192	0.875837519492
C	-0.416287432569	-1.770734651457	1.488423855744
N	-1.781504570159	-1.953294725217	1.189343094863
C	-2.204276401343	-0.888396465549	0.378668819457
C	-1.075301817081	-0.026255330989	0.167337736746
C	-1.241484791724	1.136545940443	-0.610103739672

1	C	-3.469786859283	-0.615628159849	-0.182708860341
2	C	-3.586995383548	0.529594174742	-0.947681759368
3	C	-2.483624515988	1.400560880836	-1.158284838583
4	O	4.290495922131	0.008640263777	1.014640684493
5	C	3.746696565019	-0.226384434726	-0.035905927274
6	O	4.494473592782	-0.123945856005	-1.174959127003
7	C	2.288704554866	-0.688093635351	-0.197338383689
8	N	1.849573293141	-0.355133237642	-1.577591810487
9	C	1.420327563038	-0.073795899524	0.920552797637
10	H	1.412146153708	1.034277186074	0.843824272884
11	H	1.896507396827	-0.277632254145	1.907812109970
12	H	0.121741844444	-2.466317661349	2.108743928782
13	H	-2.354593356556	-2.703693683309	1.521046329586
14	H	-0.404954594636	1.814779664362	-0.759023009239
15	H	-2.636329570348	2.293493058509	-1.761946789899
16	H	-4.310457775989	-1.280084052999	-0.013554472438
17	H	-4.544082344013	0.784258911570	-1.402640530534
18	H	2.293844678381	-1.808515421941	-0.082337832808
19	H	1.068767969275	-0.951298491104	-1.851269039141
20	H	1.506726250081	0.603909116395	-1.625891531411
21	H	3.978972655324	-0.304575832360	-2.018793497767
22				
23	**SG1**			
24	0,1			
25	C	-0.221835240588	-1.417819474945	-4.775030074593
26	C	-0.290486031974	-0.046150374144	-4.076761412792
27	O	-1.493940469045	0.620935735510	-4.467229225797
28	C	-0.220689542527	-0.153797773058	-2.537718599823
29	O	-0.772530437573	1.086511682585	-2.058942414024
30	C	-1.178069339724	-1.223476531948	-1.973342314289
31	O	-2.488967826920	-0.698168004582	-2.202227106956
32	C	-0.927142422755	-2.563935718817	-2.712599881029
33	O	-1.033642602904	-2.427120232536	-4.141138133718
34	C	1.194657069940	-2.005932130881	-4.933068259506
35	O	2.214593248346	-0.991359114334	-5.029821018185
36	C	-4.209703357948	-3.532846781735	-1.971858425236
37	C	-5.362241180707	-4.531393054696	-2.225460817112
38	O	-5.954691531641	-4.899155686211	-0.980372159934
39	C	-6.430486909271	-3.950925004432	-3.179112740814
40	C	-6.856133937673	-2.532692471171	-2.725629339613
41	O	-7.358385170054	-2.585600323062	-1.386022628217
42	C	-5.584096916537	-1.648169954667	-2.783103899313
43	O	-5.910965431196	-0.386309962899	-2.221726778579
44	O	-4.674147833272	-2.169783100582	-1.777382402167
45	C	-3.134748923557	-3.568918476244	-3.064964498429
46	O	-1.857031566778	-3.578891919068	-2.379365916155
47	C	-6.826149702951	7.545821349725	-1.120950265414

1	C	-5.498192734327	8.281539475434	-0.803390751499
2	O	-4.425421406101	7.916990223790	-1.679891968763
3	C	-4.175582460935	6.550236336989	-2.039872892819
4	C	-5.479399027601	5.778505579870	-2.344837372945
5	C	-6.582557762294	6.024803378515	-1.291978984476
6	N	-7.424760806661	8.140820195133	-2.328564218475
7	C	-8.703806647173	8.723620902857	-2.297080929657
8	O	-9.332062990177	8.795227381957	-1.258305240999
9	C	-9.184042313552	9.233802071432	-3.625357767363
10	O	-5.121212156499	8.096703267138	0.527227770631
11	C	-3.270595887967	5.865414133175	-0.993967052823
12	O	-3.246440457018	6.578128629140	0.245604935490
13	O	-7.785969918423	5.360063935416	-1.659748610929
14	C	-6.847499253297	3.065929244755	-3.352002181430
15	C	-5.394654729308	3.614588053749	-3.469698639624
16	O	-4.353610671552	2.667304791406	-3.542317649580
17	C	-4.404507062128	1.501269955428	-2.698921715235
18	C	-5.707409624985	0.770667135236	-3.081457551144
19	C	-6.947469929246	1.638520123860	-2.772238347364
20	N	-7.496484581775	3.170321246204	-4.676695271073
21	C	-8.013467141415	4.393110353469	-5.108316348395
22	O	-7.781810590431	5.427066523156	-4.486540994775
23	C	-8.787978263449	4.352715767930	-6.390000334841
24	O	-5.131422495389	4.376212575404	-2.268864093128
25	C	-4.278396593476	1.814053532770	-1.200330705528
26	O	-2.911967399962	1.876032258071	-0.800615192325
27	O	-8.074031335999	1.012273150435	-3.407333320760
28	C	-6.161464994555	-7.385015919511	-5.077380640429
29	C	-6.616295861664	-8.594612167851	-4.231475377560
30	O	-5.698858351303	-8.813012611758	-3.173557153266
31	C	-8.054472893140	-8.406076403304	-3.680522848257
32	O	-8.395901889194	-9.477464223525	-2.825640130520
33	C	-8.147874652548	-7.058860330100	-2.920561101118
34	O	-7.250736022005	-7.192483728691	-1.819087771183
35	C	-7.730104729188	-5.914298899985	-3.875498742838
36	O	-7.629818144649	-4.734319998541	-3.065287220808
37	O	-6.433801922699	-6.109085973128	-4.457371117594
38	C	-6.753587967024	-7.373271496290	-6.499717120508
39	O	-5.828577526925	-7.971351636480	-7.407293412223
40	C	3.444551030643	-1.568300392380	-1.670315483787
41	C	4.947674006644	-1.387662896489	-1.988004189926
42	O	5.468541991922	-2.577823927168	-2.555957369153
43	C	5.169867021175	-0.175424241692	-2.925437684004
44	O	6.537018674845	-0.040238812880	-3.256119330586
45	C	4.315369677968	-0.325460097915	-4.204647782040
46	O	4.811372604713	-1.488337394441	-4.887623597222
47	C	2.830407596665	-0.521512776103	-3.822502901166

1	O	2.616702294219	-1.556958998039	-2.852703807199
2	C	2.934256925550	-0.522497629070	-0.666628079041
3	O	1.677967977250	-0.930688300944	-0.111304388217
4	C	2.280100795136	3.033799606452	-2.308681199447
5	C	1.612343220956	4.379693688079	-2.677462617416
6	O	1.365123983827	4.410737776339	-4.073016882203
7	C	0.294864980143	4.617334953963	-1.893496070445
8	O	-0.345061452605	5.785080456406	-2.379640082178
9	C	-0.634321649852	3.397107142335	-2.063632153875
10	O	-0.917409857491	3.338309214733	-3.466397608839
11	C	0.104357872250	2.116301860193	-1.607002391197
12	O	1.361591610242	1.919870627744	-2.289144065409
13	C	3.051300453866	3.079926873950	-0.976873862974
14	O	4.270500168727	2.336813128241	-1.124427091048
15	H	-0.739322608036	-1.340867624369	-5.767159777361
16	H	0.502147580909	0.639601008602	-4.473452539976
17	H	-2.266117764212	0.286401984551	-3.914606031801
18	H	0.816839367047	-0.322529581984	-2.156610087041
19	H	-1.034106319099	-1.354491037766	-0.875309628753
20	H	-3.183285956746	-1.237256568905	-1.707683448243
21	H	0.051403430048	-3.021244519653	-2.436204883611
22	H	1.429927376125	-2.731529767022	-4.131407503502
23	H	1.305206322480	-2.510502604006	-5.914255056028
24	H	-3.756480378504	-3.730994022394	-0.960702569336
25	H	-4.969750644964	-5.508379284496	-2.612127394538
26	H	-6.656046818568	-4.216389271071	-0.718286684804
27	H	-6.072911402623	-3.949463418071	-4.235220980551
28	H	-7.701963162548	-2.142896990337	-3.333639788050
29	H	-6.745199013066	-2.089695781630	-0.772584987839
30	H	-5.089285602372	-1.582873758361	-3.768271696113
31	H	-3.127540502451	-4.516364221278	-3.638345556657
32	H	-3.197852755281	-2.717677354863	-3.768073799121
33	H	-7.537965438315	7.698822194992	-0.251509079417
34	H	-5.544507636811	9.388215227875	-0.942124535229
35	H	-3.597517875515	6.694152029698	-2.988730369456
36	H	-5.862292639659	6.025089033981	-3.364580690233
37	H	-6.324139931095	5.542732002253	-0.319163197697
38	H	-6.885919273621	8.076116767842	-3.187091730150
39	H	-9.194776334081	8.451211299235	-4.396511153069
40	H	-8.571395382073	10.066141328501	-3.996537788788
41	H	-10.215548698843	9.611497117816	-3.529372023954
42	H	-4.832279512705	7.147367486046	0.735763975143
43	H	-2.227682979482	5.794772076230	-1.373484553739
44	H	-3.628710634360	4.853413130488	-0.712870346255
45	H	-3.005485972975	7.534120959546	0.075342621667
46	H	-8.159663118603	5.741772257971	-2.506567508077
47	H	-7.388752629056	3.765169637302	-2.614236415660

1	H	-5.220050162557	4.232428266847	-4.380356398427
2	H	-3.486966405257	0.950070799465	-3.059726682068
3	H	-5.695057895870	0.468786703666	-4.150636925488
4	H	-7.121411331682	1.683307346839	-1.670413569059
5	H	-7.784883388621	2.290134809595	-5.107424050667
6	H	-8.227970904140	3.889549241571	-7.214414539748
7	H	-9.044673718744	5.376211224982	-6.712466104590
8	H	-9.736971099165	3.806785091883	-6.282571912200
9	H	-4.794016469050	1.045251440309	-0.591436339105
10	H	-4.664492916480	2.827943753540	-0.950556259815
11	H	-2.428321301344	1.043896087846	-1.091456194913
12	H	-8.450056956479	0.324134150460	-2.812412136739
13	H	-5.040472549065	-7.354204319801	-5.123876096238
14	H	-6.541897519192	-9.542397985356	-4.817783568987
15	H	-5.790818289667	-8.088854555774	-2.473170469322
16	H	-8.821699305646	-8.467481682442	-4.486028364339
17	H	-7.730678196507	-9.538112453947	-2.082691106899
18	H	-9.166969893757	-6.881702461259	-2.506422364144
19	H	-7.029437267400	-6.275669648281	-1.427535131826
20	H	-8.462852677064	-5.692746892860	-4.676766729107
21	H	-7.735799298327	-7.866990359565	-6.576515399633
22	H	-6.834976992231	-6.332024884888	-6.877686259357
23	H	-5.775152930484	-8.940329016702	-7.263236201931
24	H	3.252070295221	-2.611729513085	-1.313750892301
25	H	5.552250053531	-1.279221007216	-1.054656478789
26	H	5.094616931728	-2.715987842671	-3.480435508801
27	H	4.931041889736	0.787781447311	-2.401932147419
28	H	6.867030268364	-0.885750936454	-3.668617173420
29	H	4.446807186692	0.542101431693	-4.891049089403
30	H	4.131936131469	-1.780357886724	-5.555523089378
31	H	2.313468579485	0.406078346336	-3.490162455437
32	H	3.657643319596	-0.331116492060	0.145828578141
33	H	2.684565719906	0.445064105089	-1.159741503316
34	H	1.800724954455	-1.686363733280	0.500468592773
35	H	2.959677946329	2.720756221380	-3.143814879295
36	H	2.317323056037	5.233904244709	-2.534684100766
37	H	0.629417134829	3.751756392864	-4.312272585819
38	H	0.475432906091	4.847730237867	-0.819028272225
39	H	-0.471566588604	5.702257953284	-3.368585336565
40	H	-1.613484882440	3.495779710401	-1.522676388767
41	H	-1.323220077466	2.433073853951	-3.696269642301
42	H	0.266578315650	2.000290710290	-0.518998838760
43	H	3.270515678999	4.104302726647	-0.632939869995
44	H	2.515897165595	2.534628763444	-0.173055936693
45	H	4.989943719126	2.916937500698	-1.459769953422
46				
47	**SG2**			

1	0,1			
2	C	0.300920567074	-3.348555578256	-1.662323546156
3	C	-0.048926120940	-1.863344243942	-1.903387832157
4	O	-1.268569418997	-1.844445893716	-2.657385293189
5	C	-0.157358888625	-1.121014656114	-0.556540793022
6	C	-1.237747955464	-1.765604449085	0.335881569602
7	O	-2.476340712833	-1.481578384905	-0.316685585096
8	C	-0.962588195647	-3.290267012572	0.488761939211
9	O	0.120025472748	-3.763754234957	-0.284578044484
10	C	1.786409104910	-3.683988200940	-1.900608868821
11	O	1.973775232463	-4.065581495696	-3.261907315769
12	C	-4.182932993795	-4.277441296156	-0.782897352911
13	C	-4.961038375063	-5.211513032057	-1.723453787202
14	O	-6.137548674484	-5.578588492734	-0.996449707566
15	C	-5.338567221473	-4.592275256090	-3.093081616156
16	C	-5.618290530703	-3.071853799078	-3.109942459779
17	O	-6.959765312441	-2.760253739220	-2.775678998131
18	C	-4.652421895748	-2.308228972623	-2.168994800240
19	O	-5.297806318930	-1.075326821853	-1.829820263311
20	O	-4.596288135357	-2.898337922908	-0.854917095399
21	C	-2.660552824763	-4.372987915951	-0.971583715572
22	O	-2.123552998719	-4.082614831453	0.339647297175
23	C	-6.701701609537	6.964396467625	-1.743550161536
24	C	-5.696540238254	7.578633427527	-0.731973770941
25	O	-4.358940613264	7.084477518255	-0.880079125780
26	C	-4.087727421895	5.689984103988	-1.087479089174
27	C	-5.074316003090	5.061764344671	-2.094411911251
28	C	-6.544387216644	5.423245701429	-1.788377420133
29	N	-6.490730801454	7.577680741262	-3.066266005097
30	C	-7.528505792394	8.256110195002	-3.728796031646
31	O	-8.615519474193	8.402924900372	-3.204041312870
32	C	-7.162819177715	8.766071013058	-5.093743056551
33	O	-6.130191083898	7.401228753739	0.582592089723
34	C	-4.002980865344	4.928444946668	0.252231431973
35	O	-4.587585851600	5.668373491407	1.327665031793
36	O	-7.423316069129	4.834849305884	-2.733534630931
37	C	-6.094630871723	2.200747421353	-3.447943576142
38	C	-4.733294894161	2.877929693902	-3.116153779379
39	O	-3.636500760591	2.029883985208	-2.829616992535
40	C	-3.854784890062	0.888214540990	-1.971782994249
41	C	-4.941472791124	0.051398818890	-2.665533445024
42	C	-6.277980453681	0.819453994294	-2.779377982924
43	N	-6.242048185695	2.105426803032	-4.918833952204
44	C	-6.384959347600	3.255570136576	-5.692479437650
45	O	-6.186366443719	4.369329159559	-5.210054626067
46	C	-6.714793164690	3.028845382841	-7.136845466947
47	O	-4.949372832749	3.635002683863	-1.910721811194

1	C	-4.153311437717	1.266024694841	-0.514685280387
2	O	-2.930276199294	1.436266710267	0.201303342090
3	O	-7.162203819746	0.069893318177	-3.619617557487
4	C	-5.741498323617	-8.633334215086	-3.740649064994
5	C	-7.174406321303	-9.188758513074	-3.621668335693
6	O	-7.583773315447	-9.245584097624	-2.262047130060
7	C	-8.193406142705	-8.357436206058	-4.440993874906
8	O	-9.508894709723	-8.802963754251	-4.164419270026
9	C	-8.079994661665	-6.857491498745	-4.082861336334
10	C	-6.621983708064	-6.364691273393	-4.214110211653
11	O	-6.620771692840	-5.161433601741	-3.444716617849
12	O	-5.653172599549	-7.207688998925	-3.565189358922
13	C	-5.057895934565	-9.002477455369	-5.072403252189
14	O	-4.327375139441	-10.217839190173	-4.916459697836
15	C	-9.399064557534	-4.567011080250	-2.260435637311
16	C	-9.705802921615	-6.076153644378	-2.429066813664
17	O	-10.239813845789	-6.757793668805	-1.328899026312
18	C	-9.792676603390	-6.434673606116	0.016314929223
19	C	-9.785487656437	-4.920905826786	0.230233390504
20	C	-8.905387889944	-4.255734702081	-0.829376625334
21	N	-10.591263571344	-3.793754607276	-2.656644899873
22	C	-10.861056065008	-3.621094079814	-4.027432302448
23	O	-10.137380791810	-4.145969265906	-4.857962280208
24	C	-12.055083706596	-2.774863390787	-4.342708347220
25	O	-8.423309493994	-6.739784597723	-2.685685376839
26	C	-8.441944267836	-7.122062807031	0.293178009222
27	O	-8.663527508109	-8.291681364304	1.080313113154
28	O	-8.755658804936	-2.858607517679	-0.597242179491
29	C	-0.126889729219	2.542290229893	-0.396981064834
30	C	0.476081661404	1.202285984962	-0.891404533205
31	O	0.956087080974	1.168352506881	-2.216449757438
32	C	0.236787812191	1.866671343321	-3.268826841167
33	C	-0.092133280134	3.293732080298	-2.826279125702
34	C	-0.899524025130	3.278773526468	-1.520776885840
35	N	0.978599699657	3.365943671908	0.134702263050
36	C	1.312982395773	3.316288581685	1.503635729285
37	O	0.704885590341	2.584490084517	2.259664932834
38	C	2.436649165423	4.224639623595	1.906666905635
39	O	-0.592655739095	0.230822369286	-0.772290764101
40	C	-1.016542539374	1.088931644277	-3.696238214096
41	O	-0.665766253958	0.155214460203	-4.722863710691
42	O	-1.249735319599	4.609351030615	-1.146317876496
43	H	-0.346391067391	-3.998528228368	-2.299099710853
44	H	0.681777743055	-1.349967132762	-2.575993196497
45	H	-2.049047066308	-1.597567184939	-2.058021216851
46	H	0.828933759807	-1.132232940430	-0.031578943815
47	H	-1.275289122474	-1.277484920798	1.339933109921

1	H	-3.235902057274	-2.034056340868	0.071341892064
2	H	-0.645933440341	-3.572288814232	1.529101384615
3	H	2.467708179958	-2.862778442531	-1.627030578314
4	H	2.069280698732	-4.599005584677	-1.333624859456
5	H	1.904377579037	-3.288228039777	-3.855767752117
6	H	-4.464512752332	-4.501975650804	0.287929611915
7	H	-4.399706582626	-6.167416513339	-1.899522220046
8	H	-6.825510700855	-5.941565399636	-1.657736672848
9	H	-4.571435053909	-4.852963581317	-3.854760241077
10	H	-5.542512080426	-2.692275691039	-4.160185544049
11	H	-7.089516748496	-2.758037398229	-1.771032563504
12	H	-3.623608057201	-2.161178673667	-2.561594737989
13	H	-2.320849486213	-5.402403398360	-1.197770941326
14	H	-2.273330774224	-3.672288481577	-1.731931737662
15	H	-7.753652732286	7.206479929951	-1.397130363575
16	H	-5.551001220276	8.678982485188	-0.844774436564
17	H	-3.060374484416	5.740016713141	-1.542578853786
18	H	-4.810595577513	5.335216586353	-3.142050057894
19	H	-6.878978900304	4.960821134642	-0.827919743482
20	H	-5.571675457553	7.467102441282	-3.481072345075
21	H	-6.874067963150	7.955233881268	-5.776955118662
22	H	-6.342504090263	9.494426542870	-5.064729195980
23	H	-8.030483451537	9.275100227419	-5.545680496001
24	H	-6.101136390602	6.433798149754	0.888124120856
25	H	-2.946153702726	4.704240731859	0.503424533174
26	H	-4.567999211489	3.970830369222	0.243478981576
27	H	-4.192941371696	6.585414310467	1.355962665819
28	H	-7.208736710396	5.128394024025	-3.665094429264
29	H	-6.901887944862	2.903025131780	-3.037121983792
30	H	-4.337613982832	3.516209207673	-3.940493139295
31	H	-2.842568816711	0.387052802274	-2.024347339071
32	H	-4.600138342530	-0.281814049569	-3.669927166891
33	H	-6.751622095780	0.929167623983	-1.774501517456
34	H	-6.515106634892	1.182504184531	-5.273453244166
35	H	-5.998259246173	2.363141050324	-7.637794109355
36	H	-6.702498184285	3.986332296425	-7.684220636260
37	H	-7.718508228904	2.598992657520	-7.268986925717
38	H	-4.766056532881	0.486213150792	-0.020845928872
39	H	-4.641032956210	2.264266351280	-0.418008403164
40	H	-2.407050369673	0.585764919907	0.186288206328
41	H	-7.248869192872	-0.872749287786	-3.262975909526
42	H	-5.119849271193	-8.988825986233	-2.874981829187
43	H	-7.214201905460	-10.264177404060	-3.923572509504
44	H	-7.628619182468	-8.317589694068	-1.862091255337
45	H	-8.087158111643	-8.519732700580	-5.537833014562
46	H	-9.638711144576	-8.860976726484	-3.172669087212
47	H	-8.764257777000	-6.225422467003	-4.705266061583

1	H	-6.281951848886	-6.173734833178	-5.249090546436
2	H	-5.754194933520	-9.080770414564	-5.922576225140
3	H	-4.263681863840	-8.264392048711	-5.315043240883
4	H	-4.934267597707	-10.983533866478	-4.833643547687
5	H	-8.549020870958	-4.295162958946	-2.981983078991
6	H	-10.419542988309	-6.316582290563	-3.251356103438
7	H	-10.600073752182	-6.930370634049	0.613380847269
8	H	-9.408336203789	-4.669787579927	1.244511362340
9	H	-10.817982035162	-4.526729163354	0.204727555475
10	H	-7.831235061286	-4.598984864654	-0.723106301312
11	H	-11.264276984804	-3.556166600604	-1.939312253420
12	H	-11.951975582957	-1.748662413628	-3.960201209806
13	H	-12.991187441103	-3.189873885496	-3.946495376423
14	H	-12.179838457549	-2.692251247766	-5.436883872763
15	H	-7.764432905870	-6.512421155715	0.925408362294
16	H	-7.912428337350	-7.386102441184	-0.652274581010
17	H	-9.018717619235	-9.018966057019	0.522692045597
18	H	-9.560754610152	-2.349298805596	-0.817049263857
19	H	-0.859368122813	2.318478162669	0.445524379820
20	H	1.364659334261	0.873042924676	-0.305008794596
21	H	1.005894033838	1.837010370307	-4.079449433792
22	H	-0.669336295011	3.823361170485	-3.611508583740
23	H	0.836803823235	3.880898705293	-2.711535001835
24	H	-1.915658200032	2.805722624678	-1.653372754370
25	H	1.578260829729	3.822126282446	-0.544006602685
26	H	2.209667810553	5.282334386025	1.713758211693
27	H	3.382319968399	3.983572666267	1.405259279666
28	H	2.617123104227	4.135014182234	2.992701271867
29	H	-1.771748869405	1.748302937626	-4.171328042464
30	H	-1.479628763265	0.562433784786	-2.831196409276
31	H	-0.574978177494	-0.745169132103	-4.325961284829
32	H	-0.486404945175	5.115351826338	-0.804994364576
33				
34	**Phenol**			
35	0,1			
36	C	-3.931255408507	-0.706639726163	-0.008403908982
37	C	-2.533964516111	-0.680080559026	-0.023395929885
38	C	-1.844103233714	0.536300592784	-0.016257515054
39	C	-2.595850138293	1.719258958738	0.006114739499
40	C	-4.001390949730	1.720862157810	0.021907658712
41	C	-4.658352659980	0.492511570001	0.014276139050
42	H	-4.457306899801	-1.657782126779	-0.014425640227
43	H	-1.972774964741	-1.614424852469	-0.040848074863
44	H	-0.760602030882	0.558858749902	-0.027585459697
45	H	-4.540246353378	2.664517091598	0.039574205925
46	H	-5.748222630542	0.464472415835	0.026035425403
47	O	-2.010999059352	2.964482137499	0.014215339663

H	-1.024930854970	2.912319510270	0.002197890455

Benzene

0,1

C	-4.521783856749	0.866018097901	0.000071428592
C	-3.123204349210	0.865948123013	0.000498982496
C	-2.423853757865	2.077118325534	-0.000065203691
C	-3.123082674854	3.288358503458	-0.001057070816
C	-4.521662182579	3.288428479099	-0.001483874361
C	-5.221012774078	2.077258276092	-0.000919732129
H	-5.065903426800	-0.076315283965	0.000510175903
H	-2.579179449185	-0.076439702751	0.001270423281
H	-1.335709288132	2.077063881220	0.000267273910
H	-2.578963104082	4.230691884699	-0.001496280506
H	-5.065687082212	4.230816305643	-0.002255104508
H	-6.309157244254	2.077312720056	-0.001252018172

Methyl benzene

0,1

C	-2.727211747203	-0.876897960577	0.225264615998
C	-1.332996188108	-0.855018203517	0.118578412458
C	-0.656962896047	0.357556997890	-0.036502357848
C	-1.375223881304	1.563034029370	-0.086830701605
C	-2.774957322910	1.538587249946	0.021591281463
C	-3.444687177260	0.322497134334	0.176499113434
H	-3.250857175651	-1.821881893445	0.345355610846
H	-0.771035713623	-1.786731692458	0.156380524864
H	0.427380128508	0.366525128550	-0.117898310249
H	-3.339746887720	2.467140180500	-0.014571212670
H	-4.530164264443	0.309423258946	0.259488069177
C	-0.654239081500	2.863478176948	-0.238690777923
H	-1.258288311460	3.617126833061	-0.760496226691
H	-0.395437878981	3.279126974322	0.746709400323
H	0.281686487616	2.758410271754	-0.802735751301

Guassian citation:

Gaussian 16, Revision C.01,
M. J. Frisch, G. W. Trucks, H. B. Schlegel, G. E. Scuseria,
M. A. Robb, J. R. Cheeseman, G. Scalmani, V. Barone,
G. A. Petersson, H. Nakatsuji, X. Li, M. Caricato, A. V. Marenich,
J. Bloino, B. G. Janesko, R. Gomperts, B. Mennucci, H. P. Hratchian,
J. V. Ortiz, A. F. Izmaylov, J. L. Sonnenberg, D. Williams-Young,
F. Ding, F. Lipparini, F. Egidi, J. Goings, B. Peng, A. Petrone,
T. Henderson, D. Ranasinghe, V. G. Zakrzewski, J. Gao, N. Rega,
G. Zheng, W. Liang, M. Hada, M. Ehara, K. Toyota, R. Fukuda,
J. Hasegawa, M. Ishida, T. Nakajima, Y. Honda, O. Kitao, H. Nakai,

T. Vreven, K. Throssell, J. A. Montgomery, Jr., J. E. Peralta,
F. Ogliaro, M. J. Bearpark, J. J. Heyd, E. N. Brothers, K. N. Kudin,
V. N. Staroverov, T. A. Keith, R. Kobayashi, J. Normand,
K. Raghavachari, A. P. Rendell, J. C. Burant, S. S. Iyengar,
J. Tomasi, M. Cossi, J. M. Millam, M. Klene, C. Adamo, R. Cammi,
J. W. Ochterski, R. L. Martin, K. Morokuma, O. Farkas,
J. B. Foresman, and D. J. Fox, Gaussian, Inc., Wallingford CT, 2019.